PCCP

Accepted Manuscript

This article can be cited before page numbers have been issued, to do this please use: M. Villalba, M. L. Bossi and E. J. Calvo, *Phys. Chem. Chem. Phys.*, 2015, DOI: 10.1039/C5CP00225G.

ROYAL SOCIETY OF CHEMISTRY

www.rsc.org/pccp

View Article Online
DOI: 10.1039/C5CP00225G

Journal Name

RSCPublishing

ARTICLE

Cite this: DOI: 10.1039/x0xx00000x

Selective electrocatalytic hydrogenation using palladium nanoparticles electrochemically formed in Layer-by-Layer multilayer films.

M. A. Villalba,[a] M. L. Bossi,[a] E. J. Calvo,[a*]

Received 00th January 2012,
Accepted 00th January 2012

DOI: 10.1039/x0xx00000x

www.rsc.org/

Sequential adsorption of $PdCl_4^{2-}$ within weak polyelectrolyte layer-by-layer (LbL) self-assembled multilayer films with further electrochemical reduction to yield Pd^o nanoparticles (Pd-NPs) has been demonstrated. The electrocatalytic hydrogenation (ECH) of model molecules such as acetophenone and benzophenone on Pd-NPs of different size (6 to 35 nm) and bulk Pd crystal surface in hydroalcoholic acid solution has been investigated. Distribution of reaction products (secondary alcohols and alkanes) and faradaic yield was systematically investigated. While the polyelectrolyte multilayers act as nanoreactors by confining $PdCl_4^{2-}$ ions and preventing the formation of large crystals, its presence also alters the hydrogenation reaction and therefore heat treated surfaces showed only the effect of nanocrystal size on the reaction selectivity and faradaic yield.

Introduction

Modified surfaces with nanoparticles have received much attention as biocide surfaces[1, 2] and as catalysts[3, 4] for energy conversion and heterogeneous synthesis. Particularly, layer-by-layer (LbL) self-assembled films allow precursor entrapping[5-8] and limit ion free diffusion close to the electrode surface. Alternate LbL multilayer structures may act as nanoreactors enabling "*in situ*" electrocatalyst formation with electrical connectivity between nanoparticles (NPs) and the underlying substrate. For metal NPs catalyst, chemical reduction or direct electrochemical reduction[7, 9] of metal ions, completing the synthetic sequence. This exchange/reduction cycle can be repeated to increase the metal loading, i.e. the NPs size, the density of NPs on the polymeric matrix or both.

A classical reaction in organic electrochemistry is the heterogeneous hydrogenation of small organic molecules on Pd or Pt surfaces. Vago et. al[10] have employed carbon felt covered with LbL poly(allylamine)/poly(acrylic acid) multilayer film with adsorbed Pd^{2+} ions and further electroreduction to yield 6 nm Pd NPs for acetophenone hydrogenation. High selectivity towards 1-phenylethanol product was reported with Pd-NPs as compared to large Pd crystals. Product selectivity[11, 12] is of utmost importance in the synthesis of pharmaceutical compounds.

In the present work, we communicate a detailed study of Pd complex incorporation into self-assembled multilayer film with further formation of Pd-NPs on carbon felt electrodes for the hydro-genation of ketones. We report a systematic study on the influence of the polyelectrolyte matrix and the number of exchange/reduction cycles on nanoparticle size and on the resulting carbonyl group hydrogenation activity/selectivity is reported.

Experimental

Materials

Carbon felts from Morgan AM&T with a density of 0.09 g/cc and thickness 0.2 cm were cut into 1 cm diameter discs. Polyacrylic acid (PAA) (MW = 46.000) 10 wt % in water, polyallylamine (PAH) (MW= 56.000), potassium chloride and sodium hydroxide was purchased from Sigma-Aldrich. Sulfuric and hydrochloric acids were supplied by Merck. A $PdCl_2$ solution was purchased from Umicore and ethanol Sintorgan ACS 98% was used. High purity acetophenone, benzophenone, 1-phenylethanol, diphenylmethanol, ethylbenzene and diphenylmethane were supplied by Aldrich. All reagents were used as received, and the solutions were prepared with deionized water (Milli Q, 18 MΩ.cm) with unbuffered solutions of pH approximately 5.5.

Self-assembly process and metal complex uptake

A 10 MHz quartz crystal microbalance was used to quantify the polyelectrolyte mass uptake during LbL adsorption onto a negatively-charged thiolated Au electrode and further $PdCl_4^{2-}$ exchange by the multilayer film with the electrolyte. The Au coated quartz electrode was cleaned by potential repetitive cycles between 0 and 1.6 V in 0.1 M H_2SO_4 at 1 $V.s^{-1}$, followed by 0.1 $V.s^{-1}$ scan before adsorption of 1 mM 2-mercaptopropane sulfonic acid sodium (MPS).

ARTICLE View Article Online DOI: 10.1039/C5CP00225G Journal Name

The electrochemical active area was estimated by integration of the area under the gold oxide reduction peak.

The PAH/PAA LbL multistep procedure has been described elsewhere[13-15] while following the mass uptake by the QCM. The first and the outermost layer were always the polycation (PAH). All adsorptions required a stabilization and rinse step with water of the same pH as in the polyelectrolyte solution in order to take a baseline and measure the polymer effective adsorbed mass.

In the electrochemical experiments all potentials were measured and are referred herein to the Ag/AgCl; 3M KCl system (0.210 V vs. NHE) with Luggin capillary.

Preparation of Pd electrocatalyst electrodes

Prior to surface modification, the carbon felts were sonicated in isopropyl alcohol for 30 min and rinsed with copious amount of water.

Four types of modified electrodes have been used in this work: and they will be referred as **type I**, **type II**, **type I-C** and **type II-T**. In type I electrodes, Pd crystals were electrodeposited onto bare carbon felt directly from an O_2 free $PdCl_2$ electro plating bath containing 5 mM $PdCl_2$ and 0.1 M HCl at -0.20 V by passing two coulombs of charge. Type I-C electrodes were prepared as described in type I, but covered with one capping monolayer (PAH_1), three layers (PAH_2-PAA_1) or five layers (PAH_3-PAA_2) self-assembled onto the Pd crystals.

Type II Pd electrodes were prepared by building up five self-assembled layers (PAH_3-PAA_2)[5, 7] on carbon felt, with the outermost PAH layer always positively charged. Subsequently the felt was dipped for 30 minutes into a 5 mM $PdCl_2$ solution of pH 2.5 to incorporate the metal complex by ion exchange. The films were washed with copious amount of water to eliminate the unbound complex. In the final step, the Pd^{2+} ions exchanged in the polyelectrolyte film were reduced at constant -0.20 V until a charge of one coulomb has been recorded. This treatment was repeated *n* times in each case (Type II: *n*). The type II electrodes were also thermally treated at 350 ºC in an Ar atmosphere in order to burn the polyelectrolyte which aggregates the Pd-NPs (referred herein as Type II-T).

Electrosynthesis condition

Electrocatalytic hydrogenations were carried out at room temperature in a two compartment cell divided by a Nafion® 324 membrane. An Au wire was contact to the carbon felt and a platinum foil served as counter electrode.

The electrolyte was 0.1 M sulfuric acid in 60:40 ethanol-water mixture purged with Ar for a minimum of 20 minutes before each experiment.

The electrochemically active areas of the Pd surfaces were estimated by cyclic voltammetry assuming that reduction of one PdO monolayer corresponds to 420 μC.cm^{-2}[2,16, 17]. The Pd surfaces were activated by stepping the potential to -0.70 V for 120 seconds in the absence of the target molecules and then changed to -0.50 V during the injection of the organic reagent. The initial concentration of injected reactant, either ketone or alcohol, was 60 mM. The electrolysis experiments were carried out as a duplicate in order to obtain the standard deviation of each reaction. After reactant injection, the electrolyte was periodically sampled and analyzed by High Performance Liquid Chromatography (HPLC) with UV/Vis detection, using a Merk LiChroCART® 250-4 column and quantification of reactants and products was achieved using standards.

Results and Discussion

Influence of ion exchange/reduction cycles on NP size

Figure 1 shows the mass uptake as a function of time for each sequential $PdCl_4^{2-}$ exchange steps inside the ultrathin film before the subsequent reduction. First, at open circuit potential, the mass of the metal-free multilayer film increases gradually after injection of $PdCl_4^{2-}$ solution and reaches a constant value equal to 630 ng.cm^{-2} after 30 minutes followed by a potential-controlled reduction. A small mass decrease is observed after rinsing.

After the first exchange/reduction cycle, the following adsorption steps show a smaller uptake of 110 ng.cm^{-2} in each exchange. The inset in Figure 1 shows a monotonous mass increase with successive adsorption-reduction steps.

As complementary information, in Figure 1 and 2 in ESI is given the mass and the ellipsometric thickness of sequential polyelectrolyte adsorptions.

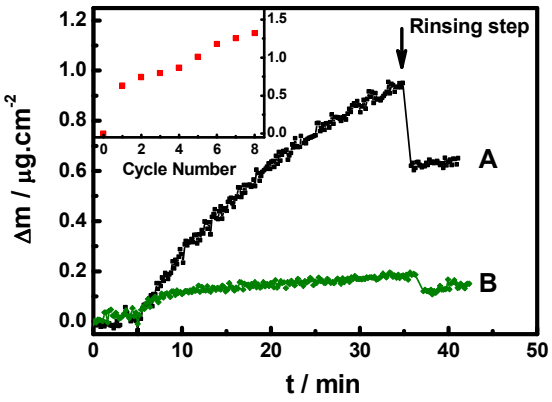

Figure 1. EQCM mass variation on Au-MPS-(PAH3-PAA2) as function of time for n = 1 (A black squares), 2 to 8 (B green) exchange/reduction cycles. Inset: incremental weight versus number of exchange/reduction cycles, n.

During ion exchange of the freshly prepared LbL polyelectrolyte, intrinsic polyion-polyion electrostatic bonds are broken and polyion-small ion bonds are formed[13, 18, 19]:

$$2Pol^{+}Pol^{-}(f) + 2H^{+}(s) + PdCl_4^{2-}(s) \rightarrow Pol_2^{+}PdCl_4^{2-}(f) + 2Pol^{-}H^{+}(f) \quad (1)$$

Thus $PdCl_4^{2-}$ ions exchanged from the electrolyte bind to NH_3^{+} groups at the surface polyelectrolyte multilayer (f), Pol^{+}, and H^{+} to Pol^{-}. The degree of complexation can be estimated from the mass of polyelectrolyte determined with the EQCM and the degree of ionization which depends on the polyelectrolyte pH

Journal Name

View Article Online
DOI: 10.1039/C5CP00225G ARTICLE

as confirmed by infrared spectroscopy (PMIRRAS) (see Figure 3 in ESI). Assuming that each $PdCl_4^{2-}$ ion is compensated by two Pol-NH_3^+, 85 % of amino groups are bound to the $PdCl_4^{2-}$ exchanged complex[20] (see Figure 4 in ESI).

During the electrochemical reduction step, Pd-NPs are formed by nucleation of Pd atoms close to the underlying electrode:

$$[(Pol^+)_2 PdCl_4^{2-}] + 2e^- \rightarrow 2(Pol^+Cl^-) + 2Cl^-(s) + Pd^0 \quad (2)$$

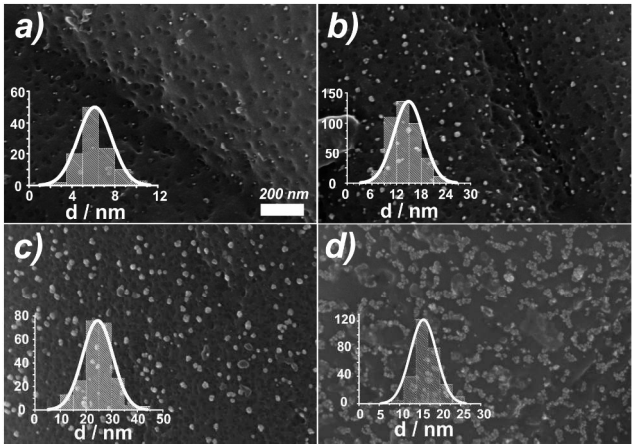

Figure 2. SEM images of type 3 modified electrodes based on different ads/red cycle number, n = a) 2, b) 4, c) 6 and d) 8. Insets: particle diameter histograms per 1.4 μm^2

Figure 2 depicts the morphology and size of the resulting Pd-NPs on a carbon fiber as shown by scanning electron microscopy (SEM) for self-assembled polyelectrolyte multilayers (type II electrodes) with increasing number of exchange/ reduction cycles (*n*). The insets show histograms of the experimental data fitted to a Gaussian function and the average values are collected in Table 1.

Table 1 Particles size, alcohol formation and Faradaic yield (FY) for electrocatalytic hydrogenation of acetophenone and benzophenone by type I and II electrodes. At total reactant conversion.

Cycle Number Type II	Diameter nm	1-phenyl ethanol % @ 500 C	FY %	Diphenyl methanol % @ 2200 C	FY %
n = 2	6.1 ± 1.6	95 ± 1	39.1 ± 5	95 ± 2	35.7 ± 6
n = 4	14.9 ± 3. 6	90 ± 2	23.0 ± 2	94 ± 1	26.5 ± 2
n = 6	24.6 ± 5.9	90 ± 2	19.2 ± 2	94 ± 2	15.0 ± 1
n = 8	49.0 ± 3.4	82 ± 2	15.2 ± 2	92 ± 2	10.8 ± 6
Type I crystals	-	84 ± 2	38.8 ± 4	78 ± 3	19.6 ± 6

The current density for the type II electrodes were comprised between 10 and 12 mA.cm^{-2} while for the type I electrodes were 3-5 mA.cm^{-2}. Also, figure 5 and 6 in ESI show the original chromatograms and calibration curves of each standard for acetophenone and benzophenone ECH. The electrodeposited Pd-NPs display quasi-spherical shapes at *n* = 2, 4 and 6 with increasing Pd-NPs diameter from 6.1 to 24.6 nm. While the smallest nanoparticles are almost totally embedded within the multilayer matrix, except in pores and holes, nanoparticles exceeding the film thickness (15-17 nm[21]) are partially uncovered and can be easily recognized. Inspection of Figure 2d shows aggregation of the individual nanoparticles probably due to the folding of the polyelectrolyte and the inhomogeneous distribution of binding sites for $PdCl_4^{2-}$. The nanoparticle clusters for *n* = 8 have an average size of 49 nm.

Unlike the nanostructures in LbL polyelectrolyte multilayer reactors (type II), palladium electrodeposits (type I) show a distinctive crystal morphology as depicted in Figure 3 with larger crystals.

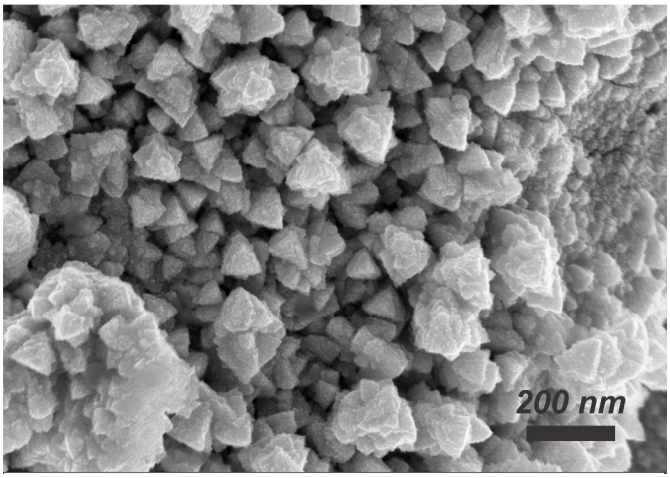

Figure 3. SEM micrograph of Pd crystals in type I electrode surfaces obtained by electrodeposition from $PdCl_4^{2-}$ at -0.20 V.

Therefore those $PdCl_4^{2-}$ ions confined inside the multilayer nanostructure, which are close enough to the underlying electrode, can be further electrochemically reduced to yield Pd-NPs unlike the freely diffusing $PdCl_4^{2-}$ ions which yield larger metal crystals by electroreduction. Further ion exchange and electroreduction steps result in larger confined crystals by growth of the former deposited particles which act as seeds.

As shown by Vago et. al. [22] with XPS and Villalba et. al. [23] with infrared spectroelectrochemistry of the exchanged redox probe hexacyanoferrate, nanoparticles are preferentially located at the film/electrode interface at tunneling distance and Pd(II) ions are coordinated in the outermost part of the film.

Surface characterization by cyclic voltammetry of type II electrodes with increasing number of cycles, *n,* is shown in ESI Figure 7. Type II electrodes exhibit a broad oxidation wave that starts at 0.55 V and a well defined peak centered at 0,42 V in the reverse scan assigned to PdO reduction. A linear increase of the total active area calculated by integration of the PdO reduction peak with the number of exchange-reduction cycles can be observed.

Selectivity of ketone electrochemical hydrogenation

The known reaction products of acetophenone hydrogenation in acidic media on Pd/graphite electrodes[24] are 1-phenylethanol, and ethylbenzene while benzophenone hydrogenation results in diphenylmethanol and diphenylmethane. The hydrogenation of ketones and alcohols can follow either a parallel[25] or sequential

ARTICLE View Article Online DOI: 10.1039/C5CP00225G Journal Name

mechanism.[13] In a recent publication[20] we have reported a detailed study of the electrocatalytic hydrogenation (ECH) of acetophenone and benzophenone on palladium electrodes. A sequential pathway of arylalkyl ketone and diaryl ketone hydrogenation via the corresponding alcohol intermediates was reported with faster kinetics for acetophenone than for benzophenone yielding a larger proportion of alcohol formation since the hydrogenation of the alcohols was found to be very slow. In the present study, the distribution of ECH products on Pd crystals (type I electrodes) and Pd-NPs (type II electrodes) are shown in Table 1 for acetophenone and benzophenone, respectively.

A decrease in the selectivity towards 1-phenylethanol production is observed as the Pd crystal size increases for the electrochemical hydrogenation of acetophenone while for benzophenone the Pd-NPs size affects the selectivity to a lesser extent. In these experiments the electrolysis was carried out to 90% ketone conversion which required ~ 500 and 2200 coulombs for acetophenone and benzophenone respectively, due to the different reactivity towards hydrogenation reaction. This also reflects in the competitive hydrogen reactions (absorption and evolution) as shown by the faradaic yield (ie. number of ketone molecules transformed per each two electrons). A slight effect on particle size has been found for acetophenone which drops with the increase of palladium crystal size. However for benzophenone no NP size effect was observed. The competition for adsorbed H atoms between recombination on adjacent Pd surface sites to yield H_2 and H atom transfer to the carbonyl group is therefore affected by the size of Pd.

Effect of the polyelectrolyte overlayers

Since Pd-NPs are partly or totally covered by the organic film we have studied the effect of the polyelectrolyte multilayer on the Pd electrode performance by deposition of one, three and five layers of polyeletrolyte on palladium deposit type I. Cyclic voltammetry of type I electrodes uncoated and coated with one, three and five polyelectrolyte layer is depicted in ESI, Figure 8. The current has been normalized by the real electrode area in order to clarify the peak shift. The effect of the LbL polyelectrolyte overlayers on Pd results in a shift of the Pd oxide reduction peak progressively towards lower potentials as would do an increase in the solution pH. This may be due to the presence of the adsorbed weak polycation (PAH).

Table 2 summarizes the distribution of reduction products and faradic yield for Pd crystals as a function of the number of adsorbed polyelectrolyte layers (type I-C).

The observed current densities for type I-C electrodes were also 3-7 $mA.cm^{-2}$, as we noted for type I electrodes. It is worth observing an increase in the alcohol production and a decrease of the faraday yield while increasing the number of LbL weak polycation (pKa ≈ 10)[20] overlayers. The LbL polymer thin film on Pd may act as a diffusion barrier for the target ketone molecules as well as blocking agent for H_{ads} active sites and immobilizer for alcohols molecules.

Table 2 Alcohol formation and Faradaic yield for ECH of acetophenone and benzophenone.

Surface	1-phenyl ethanol %	FY %	Diphenyl methanol %	FY %
Type I	84 ± 2	38.8 ± 4	78 ± 3	19.6 ± 6
Type I-C PAH_1	88 ± 1	19.2 ± 2	90 ± 3	9.0 ± 2
Type I-C PAH_2-PAA_1	90 ± 2	16.5 ± 5	90 ± 1	8.4 ± 2
Type I-C PAH_3-PAA_2	95 ± 1	10.2 ± 5	92 ± 2	4.1 ± 1

Alcohol dehydrogenation

Assuming that the hydrogenation reaction follows a sequential mechanism[26] ketone→alcohol→alkane, we have investigated the electrochemical hydrogenation of the alcohols intermediates of ketone ECH. Since this reaction is very slow as compared to the hydrogenation of the parent ketone, we have electrolyzed the system up to the same electrical charge as in the previous experiments with the respective ketones. The resulting yield of ethylbenzene and diphenylmethane and the total faraday yield are compared in Table 3. Type I and I-C exhibit low current densities (1-5 $mA.cm^{-2}$) while type II electrodes still show values between 10-15 $mA.cm^{-2}$.

Table 3 Alkane yield in ECH of 1-phenyl methanol and diphenylmethanol on Pd/PAH_3-PAA_2 (type I-C) and LbL type II electrodes.

Surface	Ethylbenzene* % @ 500 C	FY %	Diphenylmethane* % @ 2200 C	FY %
Type I	33 ± 3	14.6 ± 8	38 ± 4	4.1 ± 1
Type I-C PAH_3-PAA_2	5 ± 1	3.1 ± 2	27 ± 1	2.9 ± 2
Type II n=2	3 ± 1	1.7 ± 2	12 ± 2	1.4 ± 2

The alcohols are much less reactive than the corresponding ketones for the ECH.[20] Also, it is worth noticing the lower reactivity of diphenylmethanol towards H_{ads} on Type I electrodes with respect to 1-phenylethanol as the charge needed to reach a comparable product yield is four times larger.

The hydrocarbon concentration detected during ECH for both alcohols decreases even more for covered type II electrodes; this is particularly noticeable for ethylbenzene. The presence of the LbL multilayer films on Pd surface also results in a lower alkane yield.

The faradaic yield for the alcohols ECH on bulk Pd (type I) is lower than for the respective ketones, and for polycation covered Pd and LbL Pd-NPs is remarkably lower. Thus, most of the electrolysis results in the hydrogen reactions.

Heat treatment of the self assembled polyelectrolyte films

Heat treatment of PAH/PAA films results in cross-linking of the PAH-NH_3^+ groups and the PAA-COO^- groups at 200 ºC via amidation[27]. On the other hand, higher temperatures (700-900 ºC) pyrolyse the film and can alter metal nanoparticles size and

Journal Name
View Article Online
DOI: 10.1039/C5CP00225G
ARTICLE

morphology. Therefore, we have chosen an intermediate temperature of 350 ºC to achieve film elimination while preserving the pre-formed Pd-NPs as has been shown for poly(vinyl) alcohol stabilizer of Au nanoparticles by the Schiffrin group.[28] Infrared spectra (PM-IRRAS) of the PAH_3-PAA_2 film before and after electroreduction of confined $PdCl_4^{2-}$ ions and after heat treatment are shown Figure 3 of ESI. Elimination of the organic thin layer by heating at 350 ºC under Ar was confirmed.

Furthermore, the morphology of the palladium deposit after electroreduction shows aggregation of Pd-NPs probably induced by the polymer structure as shown in Figure 4.

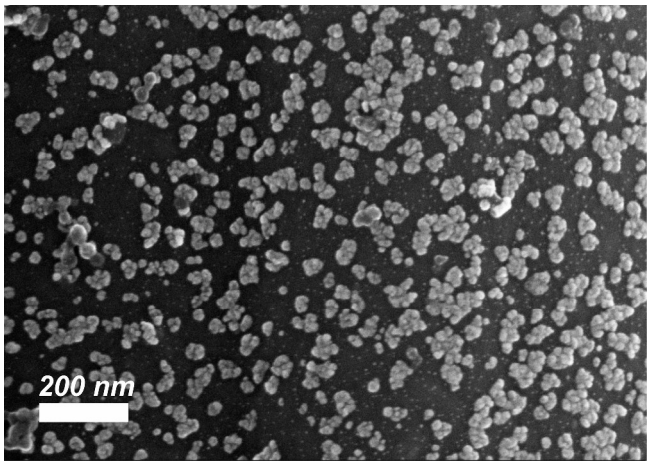

Figure 4. SEM image of type II-T with n = 8 electrode before heat treatment at 350 °C in Ar atmosphere.

However, after heat treatment at 350°C, there is a homogeneous distribution of smaller Pd-NPs as shown in Figure 5.

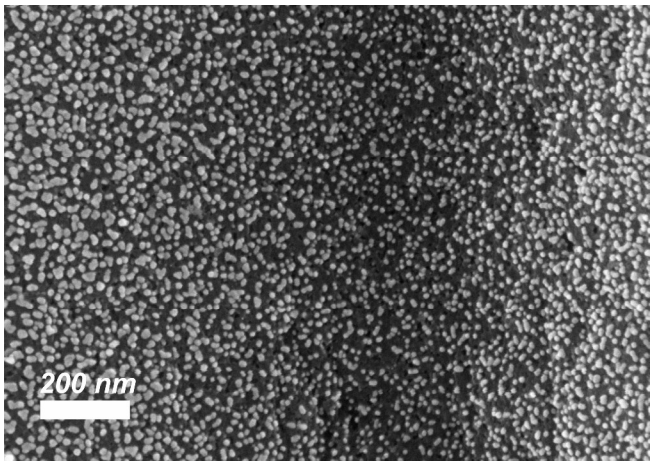

Figure 5. SEM image of type II-T with n = 8 electrode after heat treatment at 350 °C in Ar atmosphere.

To the best knowledge of the authors, the influence of the LbL polymer multilayer on the spatial distribution of confined nanoparticles has not been reported previously. The presence of the LbL structure which confines small nanoparticles also influences the cyclic voltammetry (see Figure 9 in ESI) and also the distribution of Pd NPs on the carbon felt.

Figure 6 depicts SEM images after heat treatment (type II-T) and particle size distribution. The smallest nanoparticles have an average diameter of 9 nm and they are still difficult to observe. Comparison of Figure 4 and Figure 5 also reveals an increment on particle diameter associated with the lost of aggregation and coalescence of small particles. The recovery of clean Pd NP surface after heat treatment of LbL Pd-NPs is also confirmed by cyclic as shown in Figure 7 both in the Pd oxide (A) and hydrogen (B) regions.

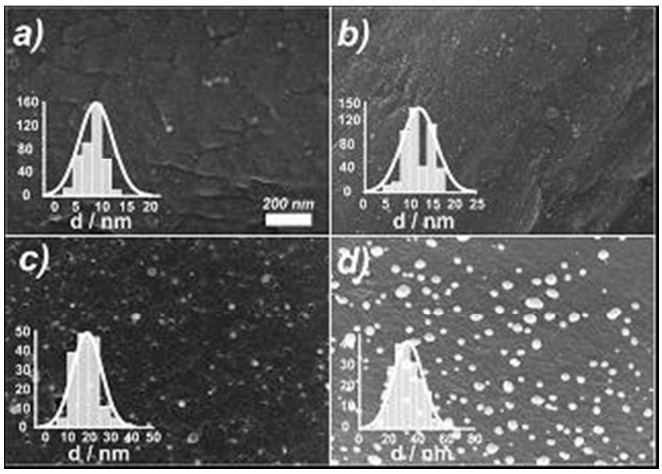

Figure 6. SEM images of type II-T at n = a) 2, b) 4, c) 6 and d) 8 after heat treatment. Insets: corresponding type II-T electrodes histograms per 1.4 μm^2

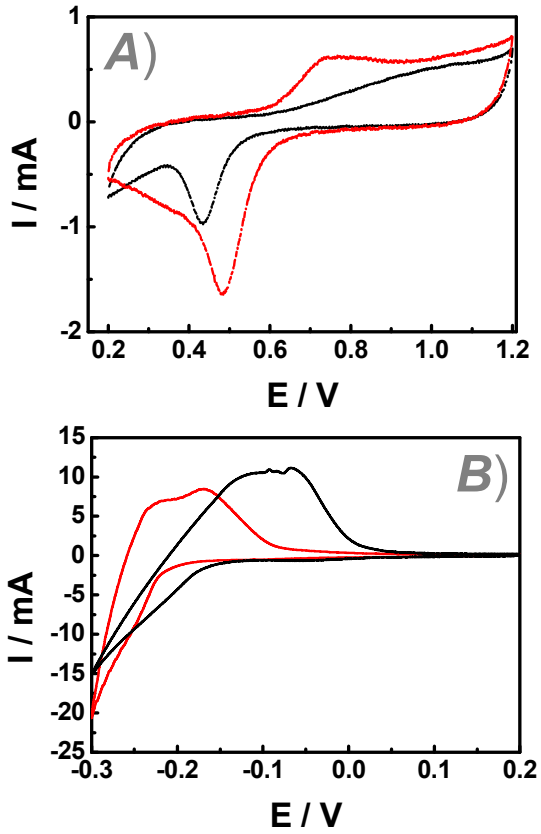

Figure 7. Cyclic voltammogram of type II-T with n = 4 electrode in 0.1 M sulfuric acid at 50 $mV.s^{-1}$, before (black line) and after heat treatment (red line).

View Article Online
DOI: 10.1039/C5CP00225G
Journal Name

For the heat treated Pd-NPs, larger electroactive area in the Pd oxide region and recovery of the Pd oxide reduction peak potential (0.49V) is apparent while better definition of the hydrogen absorption/adsorption peaks and sharper hydrogen evolution wave is also observed.

Table 4 compares the Pd-NP size, distribution of 1-phenylethanol-diphenylmethanol products and faraday yield for heat treated type II-T electrodes. Total conversion into the alcohols is observed for all Pd-NP sizes while very small faraday yield is observed in all cases, thus great competition with hydrogen evolution reaction. The observed current densities for the electrolysis experiments at -0.5 V over type II-T electrodes were comprised in the interval between 10 and 18 $mA.cm^{-2}$.

Table 4 Product distribution for ECH of acetophenone and benzophenone on heat treated type II-T electrodes at total reactant conversion.

Cycles ads/red	Diameter nm	1-phenyl ethanol %	FY %	Diphenyl methanol %	FY %
Type II-T n = 2	8.8 ± 3.5	100 ± 0	0.5 ± 2	100 ± 0	0.6 ± 2
Type II-T n = 4	12.1 ± 3.9	100 ± 0	1.2 ± 2	100 ± 0	0.6 ± 2
Type II-T n = 6	19.5 ± 6.9	100 ± 0	2.2 ± 4	100 ± 0	0.9 ± 2
Type II-T n = 8	33.6± 10.3	100 ± 0	3.1 ± 2	100 ± 0	1.5 ± 1
Type I crystals	-	84 ± 2	38.8 ± 4	78 ± 3	19.6 ± 6

After removal of the LbL film from the 9-34 nm Pd-NPs, total conversion of both ketones into the respective alcohols has been obtained with an extremely low faradaic yield. There are no differences for the increasing size of NPs in the range studied.

These results confirm those reported by Vago *et. al.*[10] for the ECH of acetophenone. This is in contrast with bare large Pd crystals with 12 to 16 % conversion into ethylbenzene and diphenylmethane.

Conclusions

The electrochemical hydrogenation (ECH) of acetophenone and benzophenone on palladium surfaces has been studied on bulk Pd electrodeposits and Pd nanoparticles confined in LbL multi-layer thin film comprised of poly (allylamine) and poly (acrylic acid).

Nanoparticle size and adsorbed polyelectrolyte on the Pd surfaces both influence the conversion of the ketones into the respective alcohols, with faster kinetics for acetophenone. On bare bulk Pd surfaces a 10-15 % conversion to the final alkane was observed, unlike on polymer coated Pd crystals.

The ECH of the respective alcohols is negligible both on Pd NPs and polymer coated Pd crystals while most of the cathodic charge results in hydrogen reactions.

Heat treatment of LbL polyelectrolyte coated NPs resulted in the elimination of the polymeric film at 350 °C as shown by FTIR spectroscopy and a distinctive cyclic voltammetry, both in the oxide and hydrogen regions. Microscopic examination of electrodeposits, before and after heat treatment, has shown that the polyelectrolyte structure determines the aggregation of palladium nanoparticles, which disperse homogeneously upon burning the polymer at 350 °C. Once the adsorbed polymer has been removed, all Pd nanoparticles in the 9-34 nm size range produced a 100 % alcohol yield for the ECH of both ketones.

Thus, we suggest that the origin of the selectivity is attributed to the blockage of the specific sites with low coordination number by polymeric matrix (4 H_{ads} transferences) and/or the exposition of new active sites for hydrogen evolution reaction after heat treatment.

Acknowledgements

MV acknowledes a PhD training fellowship of CONICET. The auhors ackowledge financial support from the University of Buenos Aires, CONICET, and ANCyPT grant PICT 2008 2037 and 2012 1452.

Electronic Supplementary Information (ESI) available: cyclic voltammetry, ellipsometry and microgravimetry for different LbL polyelectrolyte multilayers and PM-IRRAS spectroscopic data. Calibration curves of the standards of the reactions reagents and products.

References

1. J. Dai and M. L. Bruening, *Nano Letters*, 2002, 2, 497-501.
2. Z. Li, D. Lee, X. Sheng, R. E. Cohen and M. F. Rubner, *Langmuir*, 2006, 22, 9820-9823.
3. R. Raja, V. B. Golovko, J. M. Thomas, A. Berenguer-Murcia, W. Zhou, S. Xie and B. F. G. Johnson, *Chemical Communications*, 2005, 0, 2026-2028.
4. M. Liang, X. Wang, H. Liu, H. Liu and Y. Wang, *Journal of Catalysis*, 2008, 255, 335-342.
5. S. Joly, R. Kane, L. Radzilowski, T. Wang, A. Wu, R. E. Cohen, E. L. Thomas and M. F. Rubner, *Langmuir*, 1999, 16, 1354-1359.
6. T. C. Wang, M. F. Rubner and R. E. Cohen, *Langmuir*, 2002, 18, 3370-3375.
7. S. Kidambi, J. Dai, J. Li and M. L. Bruening, *Journal of the American Chemical Society*, 2004, 126, 2658-2659.
8. S. Kidambi and M. L. Bruening, *Chemistry of Materials*, 2004, 17, 301-307.
9. S. Bhattacharjee, D. M. Dotzauer and M. L. Bruening, *Journal of the American Chemical Society*, 2009, 131, 3601-3610.
10. M. Vago, M. Tagliazucchi, F. J. Williams and E. J. Calvo, *Chemical Communications*, 2008, 0, 5746-5748.
11. Y. Kashiwagi, C. Kikuchi, F. Kurashima and J.-i. Anzai, *Journal of Organometallic Chemistry*, 2002, 662, 9-13.
12. M. Vilar, J. L. Oliveira and M. Navarro, *Applied Catalysis A: General*, 2009, 372, 1-7.
13. E. J. Calvo, in *Multilayer Thin Film Sequential Assembly of Nanocomposite Materials*, ed. J. B. S. G. Decher, Wiley-VCH, Weinheim, Germany, 2012, vol. 2, ch. 42, pp. 1003-1038.

Journal Name

View Article Online
DOI: 10.1039/C5CP00225G ARTICLE

14. M. Tagliazucchi and E. J. Calvo, in *Chemically Modified Electrodes*, Wiley-VCH Verlag GmbH & Co. KGaA, 2009, pp. 57-115.
15. G. Decher, *Science*, 1997, 277, 1232-1237.
16. S. Trasatti and O. A. Petrii, *Pure Appl. Chem.*, 1991, 63, 711-734.
17. L.-l. Fang, Q. Tao, M.-f. Li, L.-w. Liao, D. Chen and Y.-x. Chen, *Chinese Journal of Chemical Physics*, 2010, 23, 543-548.
18. E. J. Calvo, in *Multilayer Thin Films. Sequential Assembly of Nanocomposite Materials*, ed. J. B. S. Gero Decher, Wiley-VCH, Weinheim, Germany, 2012, vol. 2, pp. 1003-1038.
19. J. B. Schlenoff, in *Multilayer Thin Films*, Wiley-VCH Verlag GmbH & Co. KGaA, 2012, pp. 281-320.
20. H. H. Rmaile and J. B. Schlenoff, *Langmuir*, 2002, 18, 18-20.
21. O. M. Tanchak and C. J. Barrett, *Chem. Mater. 2004*, 2004, 2734-2739.
22. N. Toshima and K. Hirakawa, *Polymer Journal*, 1999, 31, 1127-1132.
23. M. Villalba, P. M. D. Leo and E. J. Calvo, *ChemElectroChem*, 2014, 201.
24. C. M. Cirtiu, A. Brisach-Wittmeyer and H. Ménard, *Catalysis Communications*, 2007, 8, 751-754.
25. A. M. Polcaro, S. Palmas and S. Dernini, *Industrial & Engineering Chemistry Research*, 1993, 32, 1315-1322.
26. M. A. Villalba, M. Del Pozo and E. J. Calvo, *Electrochimica Acta*, 2015, In Press, Accepted Manuscript.
27. J. J. Harris, P. M. DeRose and M. L. Bruening, *Journal of the American Chemical Society*, 1999, 121, 1978-1979.
28. J. S. Jirkovsky, M. Halasa and D. J. Schiffrin, *Physical Chemistry Chemical Physics*, 2010, 12, 8042-8053.